Computational and Experimental Methods in Structures – Vol. 4

Boundary Element Methods in Engineering and Sciences

M H Aliabadi
P H Wen

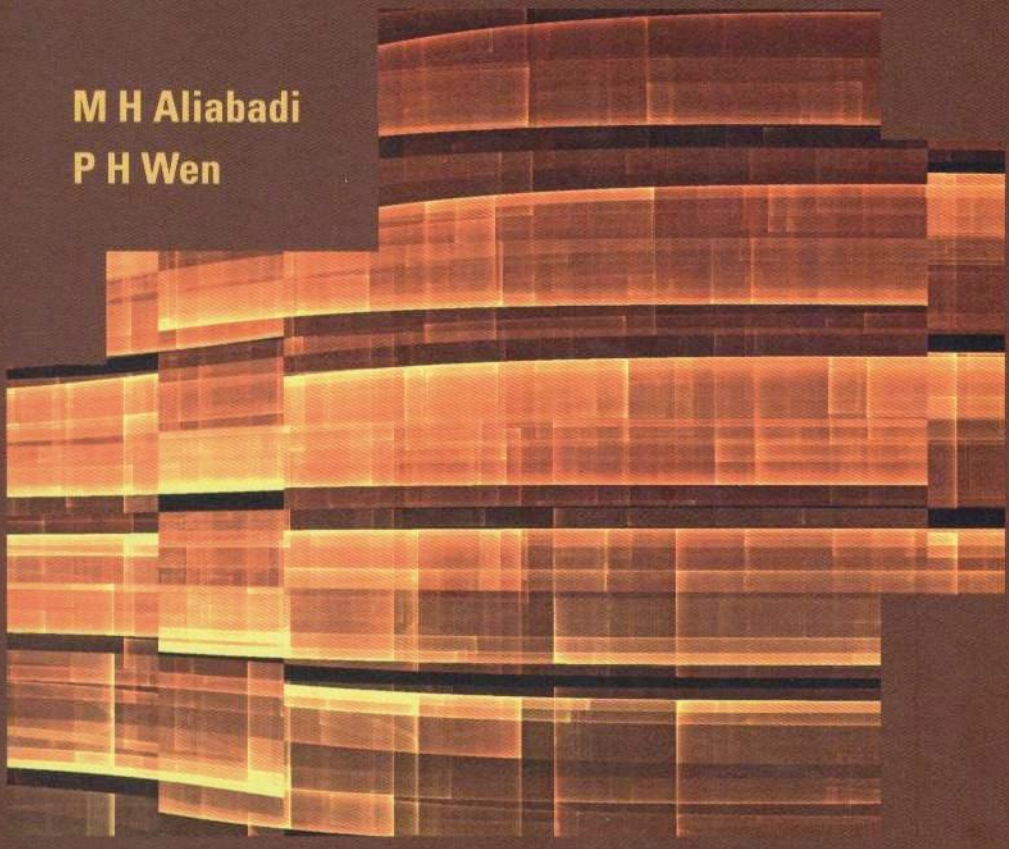

Imperial College Press

Chapter 10

CONDITION NUMBERS AND LOCAL ERRORS IN THE BOUNDARY ELEMENT METHOD

W. Dijkstra
Eindhoven University of Technology, Department of Mathematics and Computing Science, P.O. Box 513, 5600 MB Eindhoven, The Netherlands,

G. Kakuba and R.M.M. Mattheij
Mecal, P.O. Box 375, 5500 AJ Veldhoven, The Netherlands,
willemdijkstra1979@gmail.com, g.a.kakuba@tue.nl, r.m.m.mattheij@tue.nl

In this chapter we investigate local errors and condition numbers in the BEM. The results of these investigations are important in guiding adaptive meshing strategies and the solvability of linear systems in the BEM. We show that the local error for the BEM with constant or linear elements decreases quadratically with the boundary element mesh size. We also investigate better ways of treating boundary conditions to reduce the local errors. The results of our numerical experiments confirm the theory. The values of the condition numbers of the matrices that appear in the BEM depend on the shape and size of the domain on which a problem is defined. For certain critical domains, these condition numbers can even become infinitely large. We show that this holds for several classes of boundary value problems and propose a number of strategies to guarantee moderate condition numbers.

10.1. Introduction

The subject of errors in the boundary element method (BEM) is still a very interesting one and some aspects have not yet been as explored as they have been in other numerical methods like the finite element method (FEM) and the finite difference method. Errors in BEM solutions may be due to discretization or to inaccuracies in the solver that involves the use of BEM matrices with high condition numbers. For a given discretization, there are several ways to implement the BEM because of the choice in collocation and nodal points. These will all influence the resulting error

in the solution. In most cases where error measurement has been performed, like in adaptive refinement, the main focus has been a measure of the error rather than a fundamental analysis of the error and its behaviour. This chapter presents recent results on such fundamental analysis on local errors in BEM solutions. The results presented will not only be helpful in choosing an implementation strategy but also in guiding adaptive refinement techniques.

Several techniques have been used to measure BEM errors in the area of adaptive refinement. For instance, the discretization error is estimated by the difference between two solutions obtained using different collocation points but the same discretization.[1] Another technique uses the first (singular integral equation) and the second (hypersingular integral equation) kinds of formulation to provide an error estimate.[2] Data from the first kind of equation is substituted into the second kind to obtain a residual which is then used to estimate the error. Some authors have used a posteriori error estimation in FEM as a guiding tool to develop error estimates for the BEM.[3] Unfortunately, such techniques are usually restricted to the Galerkin BEM. In our case, we would like to start from the basics of the boundary integral equation (BIE) discretization to develop error analyses for collocation BEM for potential problems. Though the ideas could easily be adapted to 3-D, we will discuss 2D problems and the Laplace equation in particular.

It is well known that the Laplace equation in differential form with either Dirichlet or mixed boundary conditions has a unique solution. However, when the Laplace equation is transformed to a BIE it is not straightforward that this carries over to the BIE. It is noted that the BIE for the Dirichlet Laplace equation does not always have a unique solution.[4–7] Certain domains can be distinguished on which the BIE becomes singular and a non-trivial solution of the homogeneous equations can be found. A multiple of this solution can be added to the solution of the non-homogeneous equations, which is then no longer unique. For each domain there exists exactly one rescaled version of this domain for which the BIE becomes singular. This introduces an extraordinary phenomenon for the BIEs; uniqueness of the solutions depends on the scale of the domain.

After discretization of the boundary of the domain, the BIE transforms into a linear system of equations. When the BIE is singular, one may expect that the linear system is also singular, or at least ill-conditioned. This is reflected by the condition number of the system matrix. If this condition number is infinitely large, then the linear system is singular. As a consequence, the linear system does not have a unique solution. If the

condition number is not infinitely large, but still large, the linear system is ill-conditioned and difficult to solve. Hence the condition number also greatly affects the local error in the BEM solution. Note that it is a matter of taste to decide what 'large' means in the context of condition numbers.

The domains on which the BIE does not have a unique solution are related to the so-called *logarithmic capacity*. The logarithmic capacity is a real positive number being a function of the domain. This concept originates from the field of measure theory, but it also appears in potential theory. The concept of a capacity applied to a single domain may be a bit confusing, as usually the *electrical* capacity is defined as a charge difference between two conducting objects. The logarithmic capacity, however, is related to a single domain.

In potential theory, it is shown that when the logarithmic capacity of a domain is equal to one, then the homogeneous BIE for the Dirichlet Laplace equation on the boundary of that domain has a non-trivial solution.[8–10] This allows us to *a priori* detect whether a BIE will become singular on a certain domain. Namely, we have to compute the logarithmic capacity and verify whether it is equal to one. Additionally, the logarithmic capacity also enables us to modify the BIE such that it does not become singular. We can scale the domain in such a way that its logarithmic capacity is not equal to one. The BIE on the corresponding boundary will then be nonsingular.

The BIE for the Laplace equation with mixed boundary conditions did not receive much attention until now.[11] However, a similar phenomenon as for the Dirichlet case takes place for mixed conditions. For each domain, there exists exactly one rescaled version of this domain for which the BIE becomes singular. In this chapter, we investigate both the BIE for the Laplace equation with Dirichlet conditions and mixed conditions and the related linear systems. We also extend the research to flow problems in particular to BEM solutions of the Stokes equations.

This chapter is outlined as follows. Section 10.2 gives a recapitulation of the BEM formulation. An outline of the integral equation formulation for a Laplace problem and its discretization is presented. In Section 10.3, we present a discussion on local errors in the BEM and give the theory for the expected convergence rates of the local error for both constant and linear elements. Numerical examples and results for a Dirichlet and mixed problem are presented to illustrate the theory. Then a general insight into the various ways to implement the BEM on a circle is presented.

In Section 10.4, we give a number of illustrative examples of BEM matrices with large condition numbers. This motivates us to study the condition numbers of BEM matrices in potential problems in Section 10.5.

It is shown that these condition numbers may become infinitely large under certain conditions. This is also true for the condition numbers of BEM matrices in flow problems, which is the topic of Section 10.6. The chapter is concluded with a discussion of the results presented.

10.2. BEM Formulation for Potential Problems

In this section, we briefly present a BEM formulation. This, we do here only for potential problems but we will generalize it to Stokes equations in a later section. The BEM is used to approximate solutions of boundary value problems that can be formulated as integral equations. For the sake of clarity, we consider potential problems governed by the Laplace equation on a simply connected domain Ω in 2D with boundary Γ. That is

$$\nabla^2 u(\boldsymbol{r}) = 0, \quad \boldsymbol{r} \in \Omega. \tag{10.1}$$

We will consider problems for which either the function u (Dirichlet) or its outward normal derivative $q := \partial u/\partial n$ (Neumann) is given on Γ, or the mixed problem where on one part of the boundary u is given and on the other q is given. The integral equation formulation of (10.1) reads

$$cu + \mathcal{K}^d u = \mathcal{K}^s q, \quad \boldsymbol{r} \in \Gamma \tag{10.2}$$

Here, $\mathcal{K}^s$ and $\mathcal{K}^d$ are the *single* and *double layer operator*, defined as

$$\begin{aligned} (\mathcal{K}^s q)(\boldsymbol{r}) &:= \int_\Gamma q(\boldsymbol{r}') G(\boldsymbol{r};\boldsymbol{r}') d\Gamma_{r'}, \\ (\mathcal{K}^d u)(\boldsymbol{r}) &:= \int_\Gamma u(\boldsymbol{r}') \frac{\partial}{\partial n'} G(\boldsymbol{r};\boldsymbol{r}') d\Gamma_{r'}, \end{aligned} \tag{10.3}$$

where $\boldsymbol{r}$ and $\boldsymbol{r}'$ are points at the boundary and n' is the unit outward normal at $\boldsymbol{r}'$ at Γ. The function G,

$$G(\boldsymbol{r};\boldsymbol{r}') := \frac{1}{2\pi} \log \frac{1}{||\boldsymbol{r} - \boldsymbol{r}'||},$$

is the fundamental solution for the Laplace equation in 2D. The constant $c(\boldsymbol{r}) = 1/2$ if Γ is a smooth boundary at $\boldsymbol{r}$. Thus (10.2) expresses the potential at any point $\boldsymbol{r}$ in terms of its values $u(\boldsymbol{r}')$ and the values of its outward normal derivatives $q(\boldsymbol{r}')$ on the boundary. Some of this information will be given as boundary conditions and the rest has to be solved for. We note that the most important step of BEM is to approximate the missing

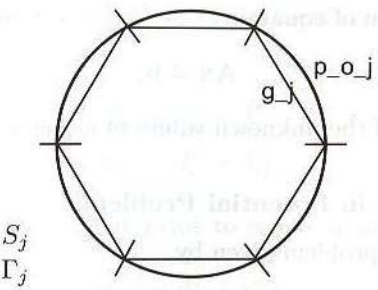

Fig. 10.1. A BEM discretization in which a polygon of rectilinear elements is used to represent a circular boundary.

boundary data as accurately as possible since the final step of computing the unknown function in Ω is merely a case of post-processing.

In a BEM discretization, the boundary Γ is divided into N partitions Γ_j such that $\cup_{j=1}^{N}\Gamma_j = \Gamma$. Each Γ_j is then represented by a numerical boundary S_j (see Fig. 10.1 for a two-dimensional case of rectilinear elements). Then on each S_j, the functions $u(\boldsymbol{r}')$ and $q(\boldsymbol{r}')$ are assumed to vary as the so-called shape functions. Let us denote these shape functions by $f_u(\xi)$ and $f_q(\xi)$, respectively, where ξ is a local coordinate on S_j. For instance, $f_u(\xi)$ and $f_q(\xi)$ are constant functions in the case of constant elements and linear functions in the case of linear elements. Thus, the discretized integral equation is

$$c(\boldsymbol{r}_i)u(\boldsymbol{r}_i) + \sum_{j=1}^{N}\int_{S_j} f_u(\boldsymbol{r}')\frac{\partial G}{\partial n'}(\boldsymbol{r}_i;\boldsymbol{r}')\,dS = \sum_{j=1}^{N}\int_{S_j} G(\boldsymbol{r}_i;\boldsymbol{r}')f_q(\boldsymbol{r}')\,dS. \tag{10.4}$$

where $\boldsymbol{r}_i$ is a node on the i-th element.

At this stage we would like to note two important sources of numerical error. First, replacing the physical boundary by a numerical boundary and second, representing the unknown functions by shape functions. The local error should be a measure of how well the solution satisfies the original integral equation on each element. In some geometries or discretization $S_j \equiv \Gamma_j$, thus eliminating one inherent source of error. The size of the local error will be small depending on how well $f_u(\xi)$ and $f_q(\xi)$ represent the original functions. Errors may also be due to integration and discontinuities at element boundaries but these can be reduced to negligible amounts by using suitable techniques. The integral equation (10.4) is written for N collocation points $\boldsymbol{r}_i$ and boundary conditions are appropriately applied to

obtain a linear system of equations

$$\mathbf{A}\mathbf{x} = \mathbf{b}, \tag{10.5}$$

where $\mathbf{x}$ is a vector of the unknown values of either u or q at the boundary.

10.3. Local Errors in Potential Problems

Consider a Dirichlet problem given by,

$$\begin{cases} \nabla^2 u(\boldsymbol{r}) = 0, & \boldsymbol{r} \in \Omega, \\ u(\boldsymbol{r}) = g(\boldsymbol{r}), & \boldsymbol{r} \in \Gamma. \end{cases} \tag{10.6}$$

The unknown in this case is the outward normal derivative $q(\boldsymbol{r}')$. Thus, what we want to solve for using BEM are the values of the normal flux at the boundary Γ; That is, $\mathbf{x} = \mathbf{q} = (q_1 \; q_2 \; \cdots \; q_N)^T$, a vector of the unknown values of $q(\boldsymbol{r}')$ at the boundary. Here we have introduced the notation

$$u(\boldsymbol{r}_i') =: u_i \quad \text{and} \quad q(\boldsymbol{r}_i') =: q_i.$$

Let $\tilde{\mathbf{q}} := (\tilde{q}_1 \; \tilde{q}_2 \; \cdots \; \tilde{q}_N)^T$ be the corresponding BEM solution and let $\mathbf{q}^* := (q_1^* \; q_2^* \; \cdots \; q_N^*)^T$ denote the exact solution at the corresponding nodes. The global error $\mathbf{e}$ is defined as

$$\mathbf{e} := \mathbf{q}^* - \tilde{\mathbf{q}}, \tag{10.7}$$

that is, pointwise,

$$e_j = q_j^* - \tilde{q}_j.$$

In order to advance our error investigations, let us define the exact values of the integrals on the j-th element from source node i as

$$I_{ij}^u := \int_{\Gamma_j} u(\boldsymbol{r}') \frac{\partial G}{\partial n'}(\boldsymbol{r}_i; \boldsymbol{r}') \, d\Gamma, \tag{10.8a}$$

$$I_{ij}^q := \int_{\Gamma_j} G(\boldsymbol{r}_i; \boldsymbol{r}') q(\boldsymbol{r}') \, d\Gamma. \tag{10.8b}$$

Let us also define the corresponding numerical estimates of (10.8) in the BEM as

$$\tilde{I}_{ij}^u := \int_{S_j} f_u(\boldsymbol{r}') \frac{\partial G}{\partial n'}(\boldsymbol{r}_i; \boldsymbol{r}') \, dS, \tag{10.9a}$$

$$\tilde{I}_{ij}^q := \int_{S_j} G(\boldsymbol{r}_i; \boldsymbol{r}') f_q(\boldsymbol{r}') \, dS. \tag{10.9b}$$

We then define the two contributions to the local error on element j due to source node i as

$$d_{ij}^q := I_{ij}^q - \tilde{I}_{ij}^q, \tag{10.10a}$$

$$d_{ij}^u := I_{ij}^u - \tilde{I}_{ij}^u. \tag{10.10b}$$

The total local error on element j due to source node i is

$$d_{ij} := d_{ij}^q + d_{ij}^u. \tag{10.11}$$

The cumulative local error for the i-th equation due to contributions from all the elements is therefore given by

$$d_i := -\sum_{j=1}^{N} d_{ij}^u + \sum_{j=1}^{N} d_{ij}^q. \tag{10.12}$$

Consider the right-hand side of the system (10.5); if we were to compute the vector $\mathbf{b}$ exactly, then the i-th component would be

$$b_i^E := -c_i u(\boldsymbol{r}_i') - \sum_{j=1}^{N} \int_{\Gamma_j} u(\boldsymbol{r}') \frac{\partial G}{\partial n}(\boldsymbol{r}_i'; \boldsymbol{r}')\, d\Gamma.$$

The one we actually use in the BEM is

$$b_i = -c_i u(\boldsymbol{r}_i') - \sum_{j=1}^{N} \int_{S_j} f_u(\boldsymbol{r}') \frac{\partial G}{\partial n}(\boldsymbol{r}_i'; \boldsymbol{r}')\, dS.$$

Let us define

$$\begin{aligned} \delta b_i := b_i^E - b_i = &-\sum_{j=1}^{N} \int_{\Gamma_j} \frac{\partial G}{\partial n}(\boldsymbol{r}_i; \boldsymbol{r}') u(\boldsymbol{r}') d\Gamma \\ &+ \sum_{j=1}^{N} \int_{S_j} f_u(\boldsymbol{r}') \frac{\partial G}{\partial n}(\boldsymbol{r}_i'; \boldsymbol{r}')\, dS = -\sum_{j=1}^{N} d_{ij}^u. \end{aligned} \tag{10.13}$$

The local error in (10.12) can therefore be expressed as

$$d_i = \delta b_i + \sum_{j=1}^{N} d_{ij}^q. \tag{10.14}$$

If the right-hand side is evaluated exactly, then $\delta b_i = 0$ and the error (10.12) would be

$$d_i = \sum_{j=1}^{N} d_{ij}^q. \tag{10.15}$$

Now, we will asses further the behaviour of these local errors.

Theorem 10.1. *The error in constant elements BEM is second order with respect to grid size.*

Proof. We need to show that the local error is third order in grid size. Take the case of an element with a Dirichlet boundary condition where the unknown is $q(\boldsymbol{r}')$. Consider the integral (10.8b), that is

$$I_{ij}^q = \int_{\Gamma_j} G(\boldsymbol{r}_i; \boldsymbol{r}') q(\boldsymbol{r}')\, d\Gamma. \tag{10.16}$$

Let l_j be the length of S_j and ξ be a local coordinate on S_j such that

$$-l_j/2 \le \xi \le l_j/2.$$

Then (10.16) is transformed and evaluated in terms of ξ. Let ξ_j be the midpoint of S_j. Suppose we have a Taylor series expansion of $q(\xi)$ about ξ_j, that is,

$$q(\xi) = q(\xi_j) + q'(\xi_j)(\xi - \xi_j) + \frac{q''(\xi_j)}{2}(\xi - \xi_j)^2 + \frac{q^{(3)}(\xi_j)}{6}(\xi - \xi_j)^3 + \cdots. \tag{10.17}$$

Then, if we use (10.17) in (10.16), we have

$$\begin{aligned} 2\pi I_{ij}^q = &\int_{-l_j/2}^{l_j/2} \ln[r(\xi)] q(\xi_j)\, d\xi + \int_{-l_j/2}^{l_j/2} \ln[r(\xi)] q'(\xi_j)(\xi - \xi_j)\, d\xi \\ &+ \int_{-l_j/2}^{l_j/2} \ln[r(\xi)] \frac{q''(\xi_j)}{2}(\xi - \xi_j)^2\, d\xi + \cdots, \end{aligned} \tag{10.18}$$

where

$$r(\xi) := \|\boldsymbol{r}_i - \boldsymbol{r}'(\xi)\|.$$

In constant elements BEM, we only use the first term, that is,

$$I_{ij}^q \approx \frac{1}{2\pi} \int_{-l_j/2}^{l_j/2} \ln[r(\xi)] q(\xi_j)\, d\xi. \tag{10.19}$$

So we have a truncation error whose principal term is the second term on the right of (10.18). Let us consider the following integral of this term,

$$I_2 := \int_{-l_j/2}^{l_j/2} q'(\xi_j) \ln[r(\xi)](\xi - \xi_j)\, d\xi. \tag{10.20}$$

We note that

$$r_1 := r(\xi = -l_j/2) \le r(\xi) \le r_2 := r(\xi = l_j/2). \tag{10.21}$$

We assume that r_i is far enough such that $r(\xi)$ remains nonzero. The distance $r(\xi)$ can be expanded about the point ξ_j as

$$r(\xi) = r(\xi_j) + r'(\xi_j)(\xi - \xi_j) + \mathrm{O}((\xi - \xi_j)^2). \tag{10.22}$$

We introduce the definitions

$$\rho_0 := r(\xi_j),$$
$$\rho_1 : + r'(\xi_j),$$

so that we can write (10.22) as

$$r(\xi) = \rho_0 \left(1 + \frac{\rho_1}{\rho_0}(\xi - \xi_j)\right) + \mathrm{O}((\xi - \xi_j)^2).$$

Then

$$\ln[r(\xi)] = \ln(\rho_0) + \frac{\rho_1}{\rho_0}(\xi - \xi_j) + \mathrm{O}((\xi - \xi_j)^2).$$

The integral I_2 can now be evaluated as

$$I_2 = \int_{-l_j/2}^{l_j/2} \ln[r(\xi)](\xi - \xi_j)\, d\xi = \int_{-l_j/2}^{l_j/2} \ln(\rho_0)(\xi - \xi_j)\, d\xi$$
$$+ \int_{-l_j/2}^{l_j/2} \left[\frac{\rho_1}{\rho_0}(\xi - \xi_j) + \mathrm{O}((\xi - \xi_j)^2)\right](\xi - \xi_j)\, d\xi. \tag{10.23}$$

Since we use the midpoint as ξ_j, the first integral on the right of (10.23) is zero so that we remain with

$$I_2 = \int_{-l_j/2}^{l_j/2} \frac{\rho_1}{\rho_0}(\xi - \xi_j)^2\, d\xi + \mathrm{O}((\xi - \xi_j)^5). \tag{10.24}$$

Then using the mean value theorem,

$$I_2 \approx \frac{\rho_1}{\rho_0}(\zeta - \xi_j)^2 l_j \quad \zeta \in (-l_j/2,\ l_j/2). \tag{10.25}$$

For ξ_j a midpoint of S_j

$$|\zeta - \xi_j| \leq l_j/2. \tag{10.26}$$

Putting (10.25) and (10.26) together we have

$$|I_2| \leq \frac{l_j^3}{4}|\rho_1/\rho_0|,$$

which is third order in grid size. This shows that constant elements BEM can be expected to be of second order. □

Theorem 10.2. *The error in linear elements BEM is second order with respect to grid size.*

Proof. Likewise, we need to show that the local error is third order in grid size. In linear elements, the unknown function is assumed to vary linearly on the element, that is,

$$q(\xi) \approx p_1(\xi) := \alpha_0 + \alpha_1 \xi,$$

where α_0 and α_1 are constants and ξ a local coordinate on S_j. The error in this case is due to the error when we interpolate by an order one polynomial which is given by[12]

$$q(\xi) - p_1(\xi) = \frac{q''(\eta)}{2}(\xi - \xi_0)(\xi - \xi_1), \quad \eta \in (\xi_0, \xi_1).$$

Using this result, the local error in BEM will be

$$E_{s_1} = \frac{1}{4\pi}\int_{-l_j/2}^{l_j/2} \ln[r(\xi)]q''(\eta)(\xi - \xi_0)(\xi - \xi_1)\,d\xi, \tag{10.27}$$

where ξ_0 and ξ_1 are the interpolation coordinates. Again using the second mean value theorem, we have

$$\begin{aligned} E_{s_1} &\approx \frac{\ln[r(\beta)]q''(\eta)}{4\pi}\int_{-l_j/2}^{l_j/2}(\xi - \xi_0)(\xi - \xi_1)\,d\xi \\ &= -\frac{l_j^3}{24\pi}\ln[r(\beta)]q''(\eta), \end{aligned} \tag{10.28}$$

where $\xi_0 = -l_j/2$, $\xi_1 = l_j/2$ and β is an intermediate point. This result shows that linear elements BEM can be expected to be of second order. □

10.3.1. *Numerical examples*

In this section we will perform numerical experiments to illustrate the above claims about the error. Results show that indeed we obtain second order convergence of the error. Our experiments are performed on a circle which rules out the errors caused by discontinuities at corners in other geometries like a square. It would be a natural choice to work on a unit circle but in our examples we avoid this choice for reasons that will become clear in later sections.

Example 10.3.1. Consider the boundary value problem

$$\begin{cases} \nabla^2 u(\boldsymbol{r}) = 0, & \boldsymbol{r} \in \Omega := \{\boldsymbol{r} \in \mathbb{R}^2 : ||\boldsymbol{r}|| \leq 1.2\}, \\ u(\boldsymbol{r}) = g(\boldsymbol{r}'), & \boldsymbol{r} \in \Gamma. \end{cases} \tag{10.29}$$

The boundary condition function $g(\boldsymbol{r}')$ is chosen such that the exact solution is

$$q(\boldsymbol{r}') = \frac{(\boldsymbol{r}' - \boldsymbol{r}_s) \cdot \boldsymbol{n}(\boldsymbol{r}')}{||\boldsymbol{r}' - \boldsymbol{r}_s||^2}, \tag{10.30}$$

where the source point $\boldsymbol{r}_s = (0.36, 1.8)$ is a fixed point outside Ω and $\boldsymbol{n}(\boldsymbol{r}')$ is the outward normal at $\boldsymbol{r}'$.

We will use this example to verify the results of theorems 10.1 and 10.2. Since we have the analytic expression for the unknown $q(\boldsymbol{r}')$ we can compute the global error in (10.7). As we see in Tables 10.1 and 10.2, the results show that indeed the error for both constant and linear elements exhibits second order behaviour.

In Table 10.1, we discretize as in Fig. 10.1 using an inscribed regular polygon of N sides. We refine by a factor of three because we are using constant elements with the midpoints as nodes and we would like to compute the pointwise error as shown in the second column. For a better

Table 10.1. Errors to the Dirichlet problem (10.29) using constant elements BEM with rectilinear elements.

N	$e_j = \lvert q_j^* - \tilde{q}_j \rvert$	$\lVert \mathbf{e} \rVert_2 / \sqrt{N}$	$e_j(N)/e_j(3N)$
5	6.57E-02	2.80E-01	8.66
15	7.58E-03	3.53E-02	9.43
45	8.04E-04	5.40E-03	9.12
135	8.82E-05	6.58E-04	9.04
405	9.76E-06	7.53E-05	9.01
1,215	1.08E-06	8.45E-06	9.00
3,645	1.20E-07	9.42E-07	—

Table 10.2. Errors to the Dirichlet problem (10.29) using linear elements BEM.

N	$e_j = \lvert q_j^* - \tilde{q}_j \rvert$	$\lVert e \rVert_2 / \sqrt{N}$	$e_j(N)/e_j(3N)$
5	1.39E-02	1.29E-01	70.1
15	1.98E-04	2.11E-02	12.9
45	1.53E-05	4.89E-03	10.7
135	1.42E-06	6.07E-04	9.6
405	1.47E-07	7.00E-05	9.2
1,215	1.59E-08	7.88E-06	9.2
3,645	1.72E-09	8.79E-07	—

comparison, we use the same refinement factor for linear elements as well. Both the pointwise error and the median 2-norm of the error show the same trend of error convergence. The pointwise error is computed at the point $\boldsymbol{r}' = (-0.370820, -1.141268)$ on the circle. As we can see from the ratios of consecutive errors, the convergence is second order.

A discretization using arcs instead of rectilinear elements as shown in Fig. 10.2 gives similar results, see Table 10.3.

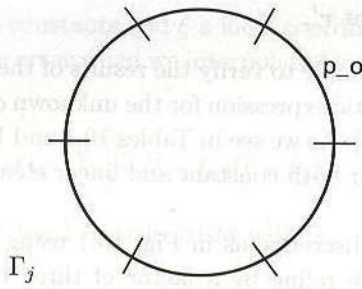

Fig. 10.2. A BEM discretisation of a circle using circular arcs.

Table 10.3. Errors to Dirichlet problem (10.29) when we use constant elements BEM with circular arc elements.

N	$\lvert e_j \rvert = \lvert q_j^* - \tilde{q}_j \rvert$	$\lVert e \rVert_2 / \sqrt{N}$	$e_j(N)/e_j(3N)$
5	5.54E-03	1.44E-001	13.6
15	4.06E-04	1.25E-002	10.8
45	3.77E-05	2.55E-003	9.6
135	3.94E-06	3.55E-004	9.2
405	4.28E-07	4.21E-005	9.1
1,215	4.72E-08	4.78E-006	9.0
3,645	5.23E-09	5.34E-007	—

Example 10.3.2. Consider the Neumann boundary value problem

$$\begin{cases} \nabla^2 u(\boldsymbol{r}) = 0, & \boldsymbol{r} \in \Omega := \{\boldsymbol{r} \in \mathbb{R}^2 : ||\boldsymbol{r}|| \leq 1.2\}, \\ q(\boldsymbol{r}) = h(\boldsymbol{r}'), & br \in \Gamma. \end{cases} \tag{10.31}$$

The boundary condition function $h(\boldsymbol{r}')$ is chosen such that the exact solution is

$$u(\boldsymbol{r}') = \log(||\boldsymbol{r}' - \boldsymbol{r}_s||), \tag{10.32}$$

where the source point $\boldsymbol{r}_s = (0.36, 1.8)$ is a fixed point outside Ω and $\boldsymbol{n}(\boldsymbol{r}')$ is the outward normal at $\boldsymbol{r}'$. In the implementation, a Dirichlet boundary condition is prescribed at the last node $j = N$ as a remedy to obtain a well posed problem. So, in actual sense, we solve a mixed boundary problem. We also compute the pointwise and median 2-norm errors and the results are shown in Table 10.4. The convergence behaviour is the same as that for the Dirichlet problem. Both errors show a second order convergence as we can see from the ratios of consecutive errors.

10.3.2. *A detailed study of local errors*

As mentioned earlier, the freedom to choose collocation points for a given discretization suggests that there are several ways to implement the BEM. In this section we survey the possibilities but restrict ourselves to a circular domain.

Suppose we use rectilinear elements to discretize the circle such that the numerical boundary is a polygon like the one shown in Fig. 10.3. Besides, the way we treat the boundary conditions is also very important as we will see in the survey that follows.

In the usual constant elements formulation, the nodes are the midpoints of the elements and also function as the collocation points. For the

Table 10.4. Errors to the mixed (one Neumann boundary node) problem using constant elements BEM.

N	$\lvert e_j\rvert = \lvert u_j^* - \tilde{u}_j\rvert$	$\lVert\mathbf{e}\rVert_2/\sqrt{N}$	$e_j(N)/e_j(3N)$
5	1.39E-01	4.66E-01	23.5
15	5.92E-03	2.25E-02	13.0
45	4.55E-04	2.88E-03	8.7
135	5.24E-05	3.27E-04	8.9
405	5.89E-06	3.65E-05	9.0
1,215	6.57E-07	4.07E-06	9.0
3,645	7.31E-08	4.52E-07	—

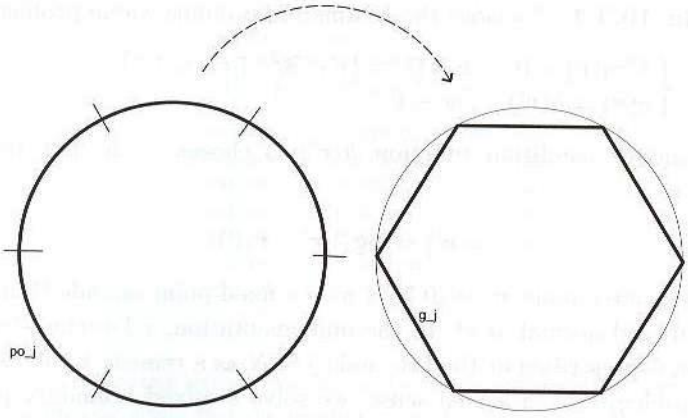

Fig. 10.3. Discretizsation of a circle by a six element polygon.

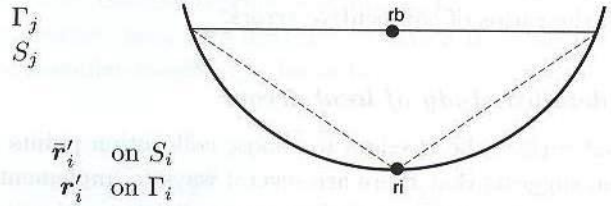

Fig. 10.4. Numerical representation of boundary points; r'_i the exact point and $\bar{r}'_i$ its numerical representation.

discretization shown in Fig. 10.3, the numerical boundary does not coincide with the physical boundary and therefore we can talk of exact points r'_i and their numerical representations $\bar{r}'_i$ as shown in Fig. 10.4. Since our goal is to come up with a proper understanding of (local) errors for the BEM, we would like to explore the various possibilities we have to choose the collocation points and nodes. These possibilities are summarized in Table 10.5.

As mentioned earlier, it is important to differentiate between nodal points (the points used to approximate the functions) and the collocation points (the points where the integral equation is applied). Nevertheless, the boundary condition on S_i shown in Fig. 10.4 is $u(r'_i)$. We consider again the Dirichlet problem, (10.29), and compute errors for some of the numbered cases in the table. Similar to the examples of the previous section, the pointwise error is computed at the point $(-0.370820, -1.141267)$.

Table 10.5. Summary of possibilities on implements of constant elements BEM on a circle.

Collocation on S_j	u constant	integration of b on S_j	integration of A on S_j	(1)
			integration of A on Γ_j	
		integration of b on Γ_j	integration of A on S_j	(2)
			integration of A on Γ_j	
	u exact	integration of b on S_j	integration of A on S_j	(3)
			integration of A on Γ_j	
		integration of b on Γ_j	integration of A on S_j	(4)
			integration of A on Γ_j	
Collocation on Γ_j	u constant	integration of b on S_j	—	
			—	
		integration of b on Γ_j	—	
			integration of A on Γ_j	(5)
	u exact	integration of b on S_j	—	
			—	
		integration of b on Γ_j	—	
			integration of A on Γ_j	(6)

Case (1) in Table 10.5 is the traditional constant elements BEM, that is, on S_j, u is constant and given by $\bar{u}_j := u(\boldsymbol{r}'_j)$. For the linear system of equations, we have,

$$b_i = -c_i \bar{u}_i - \sum_{j=1}^{N} \int_{S_j} \bar{u}_j \frac{\partial G}{\partial n'}(\bar{\boldsymbol{r}}'_i; \boldsymbol{r}')\, dS,$$

$$A_{ij} = -\int_{S_j} G(\bar{\boldsymbol{r}}'_i; \boldsymbol{r}')\, dS.$$

In case (3) in the table, we have the 'exact' right-hand side. But it is not yet really exact because we integrate on S_j, and not Γ_j thus the boundary function is evaluated on the numerical boundary. The difference now is that we make no assumptions on the given boundary function u. That is,

$$b_i = -c_i u(\boldsymbol{r}'_i) - \sum_{j=1}^{N} \int_{S_j} u(\boldsymbol{r}') \frac{\partial G}{\partial n'}(\bar{\boldsymbol{r}}'_i; \boldsymbol{r}')\, dS,$$

$$A_{ij} = -\int_{S_j} G(\bar{\boldsymbol{r}}'_i; \boldsymbol{r}')\, dS.$$

Case (5) is like the traditional BEM but with the integrations carried out on the arcs. The fixed point i is on the arc and the functions $u(\boldsymbol{r})$ and

$q(\boldsymbol{r})$ are assumed constant on each element j.

$$b_i = -c_i \bar{u}_i - \sum_{j=1}^{N} \int_{\Gamma_j} \bar{u}_j \frac{\partial G}{\partial n'}(\boldsymbol{r}_i'; \boldsymbol{r}')\, dS,$$

$$A_{ij} = -\int_{\Gamma_j} G(\boldsymbol{r}_i'; \boldsymbol{r}')\, dS.$$

In case (6) we integrate the exact boundary function $u(\boldsymbol{r})$ as given. Thus we use 'the exact right-hand side'

$$b_i = -c_i u(\boldsymbol{r}_i') - \sum_{j=1}^{N} \int_{\Gamma_j} u(\boldsymbol{r}') \frac{\partial G}{\partial n'}(\boldsymbol{r}_i'; \boldsymbol{r}')\, dS,$$

$$A_{ij} = -\int_{\Gamma_j} G(\boldsymbol{r}_i'; \boldsymbol{r}')\, dS.$$

We expect that the results of case (3) are better than those of case (1) since case (3) should capture the variation of the boundary function better. For the same reasons, the results of case (6) are expected to be better than those of case (5). Since in cases (5) and (6) the numerical boundary coincides with the physical boundary, the corresponding results should be better than those of cases (1) and (3).

Comparing the results in Tables 10.6 and 10.7, we see that indeed we obtain better results in case (3) than in case (1). The gain is not much in this example and this is because of the smooth variation of the boundary condition function on the large part of the boundary. This also explains the small difference between the results in Tables 10.8 and 10.9. As we expected, the results of cases (5) and (6) are better than those of cases (1) and (3) respectively. We see that the pointwise errors in Table 10.8 are at least one order smaller than those in Table 10.6.

Table 10.6. Errors for case (1) in Table 10.5.

N	$\lvert e_j \rvert = \lvert q_j^e - \tilde{q}_j \rvert$	$\lVert \mathbf{e} \rVert_2 / \sqrt{N}$
5	6.57E-02	2.81E-01
15	7.58E-03	3.53E-02
45	8.04E-04	5.40E-03
135	8.82E-05	6.58E-04
405	9.76E-06	7.53E-05
1,215	1.08E-06	8.45E-06
3,645	1.20E-07	9.42E-07

Table 10.7. Errors for case (3) in Table 10.5.

N	$\lvert e_j\rvert = \lvert q_j^e - \tilde{q}_j\rvert$	$\lVert\mathbf{e}\rVert_2/\sqrt{N}$
5	3.01E-01	4.57E-01
15	4.57E-03	2.17E-02
45	4.76E-04	3.70E-03
135	5.20E-05	4.73E-04
405	5.74E-06	5.49E-05
1,215	6.37E-07	6.19E-06
3,645	7.07E-08	6.91E-07

Table 10.8. Errors for case (5) in Table 10.5.

N	$\lvert e_j\rvert = \lvert q_j^e - \tilde{q}_j\rvert$	$\lVert\mathbf{e}\rVert_2/\sqrt{N}$
5	5.54E-03	1.44E-01
15	4.06E-04	1.25E-02
45	3.77E-05	2.55E-03
135	3.94E-06	3.55E-04
405	4.28E-07	4.21E-05
1,215	4.72E-08	4.78E-06
3,645	5.23E-09	5.34E-07

Table 10.9. Errors for case (6) in Table 10.5.

N	$\lvert e_j\rvert = \lvert q_j^e - \tilde{q}_j\rvert$	$\lVert\mathbf{e}\rVert_2/\sqrt{N}$
5	2.96E-02	1.59E-01
15	4.05E-04	1.24E-02
45	3.62E-05	2.40E-03
135	3.88E-06	3.49E-04
405	4.26E-07	4.19E-05
1,215	4.31E-08	4.77E-06
3,645	1.66E-08	5.34E-07

10.4. Large Condition Numbers

In all practical applications of the BEM, a linear system needs to be solved eventually. In most cases it is assumed that the condition number of the system matrix is moderate, i.e. the linear system has a unique solution and can be solved accurately. However, it is not very clear if this is always true.

It is known that the condition number of the BEM matrix in potential problems with Dirichlet conditions depends on the size and shape of the domain on which the potential problem is defined.[4–7] On most domains

the condition number is moderate, but on certain domains the condition number becomes infinitely large.

When the BEM is applied to the Laplace equation with Dirichlet conditions on a circular domain, the condition number of the BEM matrix can be computed analytically.[13,14] Here, rectilinear elements are used and a constant approximation of the functions at each element. It can be shown that the condition number depends on the radius R of the circle and the number of boundary elements N according to

$$\mathrm{cond}(\mathbf{G}) = \frac{\max\left(\frac{1}{2}, |\log R|\right)}{\min\left(\frac{1}{N}, |\log R|\right)}. \tag{10.33}$$

This leads to the observation that the condition number is infinitely large when the radius of the circle is equal to one. Hence, the size of the domain affects the condition number of the BEM matrix and, consequently, it also affects the solvability of the linear system. This introduces a remarkable phenomenon: the solvability of a linear system in the BEM depends on the size of the domain.

For the potential problem with Neumann conditions the corresponding BEM matrix is always infinitely large, since this problem is ill-posed, regardless of the size and shape of the domain. The question then arises whether we may expect infinitely large condition numbers when solving potential problems with mixed boundary conditions. In this case, the BEM matrix is a composite matrix, consisting of a number of columns from the Dirichlet BEM matrix, and a number of columns from the Neumann BEM matrix. The first matrix is ill-conditioned on some domains, the latter is ill-conditioned always. It is not clear how this affects the condition number of the composite matrix.

For the Laplace equation with mixed conditions on a circular domain, it is possible to give an estimate for the BEM matrix.[15] Again, it shows that for the unit circle the condition number is infinitely large. Hence, the mixed problem seems to inherit the solvability problem from the Dirichlet problem.

Figures 10.5 and 10.6 correspond to solving the Laplace equation on a triangular domain and an ellipsoidal domain, respectively. The size of the triangle is characterized by its side length l, whereas the ellipse is characterized by the lengths of the semi-axes a and $a/2$. We show the condition numbers for the Dirichlet BEM matrix (squares) and the mixed BEM matrix (circles). For the mixed problem, we set the number of boundary elements with Dirichlet conditions equal to the number of

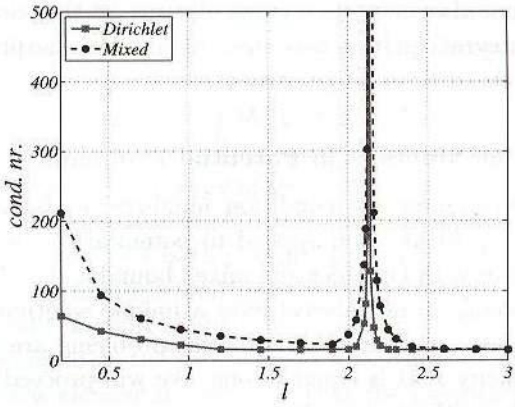

Fig. 10.5. The condition number of the matrices **A** (circles) and **G** (squares), corresponding to the Laplace equation with mixed boundary conditions and Dirichlet boundary conditions, respectively, for a triangular domain.

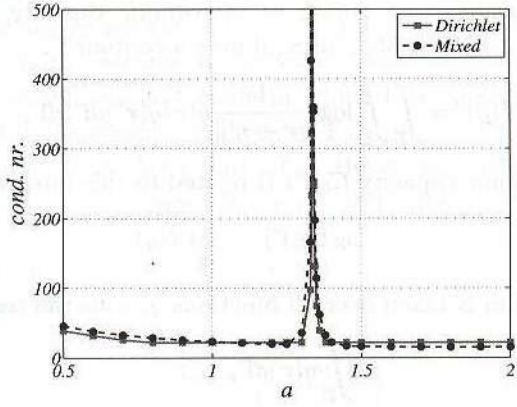

Fig. 10.6. The condition number of the matrices **A** (circles) and **G** (squares), corresponding to the Laplace equation with mixed boundary conditions and Dirichlet boundary conditions, respectively, for an ellipsoidal domain.

boundary elements with Neumann conditions. Again, we see that the condition numbers are infinitely large for certain sizes of the domains. Hence, again the size of the domain influences the solvability of the linear systems in the BEM.

In the next section, we present the theory behind this remarkable phenomenon by studying the boundary integral equations that lay the foundations of the BEM. We show that, regardless of the shape of

the domain, there always exists a particular size of that domain for which the boundary integral equation becomes singular. We also propose a number of strategies to avoid these singularities.

10.5. Condition Numbers in Potential Problems

This section investigates the condition numbers of the system matrices that appear in the BEM when applied to potential problems. We analyse potential problems with Dirichlet and mixed boundary conditions and show that these problems do not always have a unique solution. This happens when the domains on which the potential problems are defined have a logarithmic capacity that is equal to one. We will proceed by introducing the concept of logarithmic capacity.

10.5.1. *Logarithmic capacity*

To study the uniqueness properties of the Dirichlet and the mixed problem, we need to introduce the notion of *logarithmic capacity*. We define the energy integral I by a double integral over a contour Γ,

$$I(q) := \int_\Gamma \int_\Gamma \log \frac{1}{\|\boldsymbol{r} - \boldsymbol{r}'\|} q(\boldsymbol{r}) q(\boldsymbol{r}') d\Gamma_r d\Gamma_{r'}, \tag{10.34}$$

and the logarithmic capacity $C_l(\Gamma)$ is related to this integral by

$$-\log C_l(\Gamma) := \inf_q I(q). \tag{10.35}$$

Here, the infimum is taken over all functions q, with the restriction that

$$\int_\Gamma q(\boldsymbol{r}) d\Gamma_r = 1. \tag{10.36}$$

Let us give a physical interpretation of the logarithmic capacity. For simplicity, let the domain Ω be contained in the disc with radius $1/2$. In that case, it can be shown that the integral $I(q)$ is positive. The function q can be seen as a charge distribution over a conducting domain Ω. Faraday demonstrated that this charge will only reside at the exterior boundary of the domain ('cage'), in our case at Γ. We normalize q in such a way that the total amount of charge at Γ is equal to one, cf. condition (10.36). The function

$$\frac{1}{2\pi} \int_\Gamma \log \frac{1}{\|\boldsymbol{r} - \boldsymbol{r}'\|} q(\boldsymbol{r}') d\Gamma_{r'} \equiv (\mathcal{K}^s q)(\boldsymbol{r}) \tag{10.37}$$

is identified as the potential due to the charge distribution q. Note that the integral I can also be written as

$$I(q) = 2\pi \int_\Gamma (\mathcal{K}^s q)(\boldsymbol{r}) q(\boldsymbol{r}) d\Gamma_r. \tag{10.38}$$

Hence, I can be seen as the energy of the charge distribution q. The charge will distribute itself over Γ in such a way that the energy I is minimized, so the quantity $-\log C_l(\Gamma)$ is the minimal amount of energy. Hence, the logarithmic capacity $C_l(\Gamma)$ is a measure for the capability of the boundary Γ to support a unit amount of charge.

For most boundaries the logarithmic capacity is not known explicitly. It is only for a few elementary domains that the logarithmic capacity can be calculated analytically[9]; we have listed some in Table 10.10.

There are also some useful properties that help us to determine or estimate the logarithmic capacity.[8,16]

(1) If Γ is the outer boundary of a closed bounded domain Ω, then $C_l(\Gamma) = C_l(\Omega)$. This agrees with the idea of Faraday's cage, mentioned above.
(2) Denote by d_Γ the Euclidean diameter of Ω, then $C_l(\Gamma) \leq d_\Gamma$. Hence, the radius of the smallest circle in which Γ is contained is an upper bound for the logarithmic capacity of Γ.
(3) If $\Gamma = \boldsymbol{x} + \alpha\Gamma_1$, then $C_l(\Gamma) = \alpha C_l(\Gamma_1)$. Hence, the logarithmic capacity behaves linearly with respect to scaling and is invariant with respect to translation.
(4) If $\Omega_1 \subset \Omega_2$, then $C_l(\Omega_1) \leq C_l(\Omega_2)$.
(5) For a convex domain Ω,

$$C_l(\Omega) \geq \left(\frac{\text{area}(\Omega)}{\pi}\right)^{1/2}. \tag{10.39}$$

Table 10.10. The logarithmic capacity of some domains. Note that $\Gamma(\cdot)$ represents the gamma-function.

Boundary Γ	Logarithmic capacity
circle with radius R	R
square with side L	$\frac{\Gamma(\frac{1}{4})^2}{4\pi^{3/2}} L \approx 0.59017 \cdot L$
ellipse with semi-axes a and b	$(a+b)/2$
interval of length a	$\frac{1}{4}a$
isosceles right-angled triangle side l	$\frac{3^{3/4}\Gamma(1/4)^2}{2^{7/2}\pi^{3/2}}\, l \approx 0.476\, l$

If the properties from the list above do not supply accurate enough estimates, the logarithmic capacity can also be approximated numerically with the help of linear programming[17] or using the BEM-matrices explicitly.[18]

10.5.2. *Dirichlet problem*

We consider the Laplace equation (10.1) with Dirichlet boundary conditions, with corresponding BIE (10.2). For the single layer operator $\mathcal{K}^s$ in this BIE we have the following result.

Theorem 10.3. *There exists a nonzero q_e such that*

$$(\mathcal{K}^s q_e)(\boldsymbol{r}) = -\frac{1}{2\pi} \log C_l(\Gamma), \quad \boldsymbol{r} \in \Gamma. \tag{10.40}$$

Sketch of proof. In the following, we briefly present the major steps in the proof of the theorem.[8,19,20] We observe that the energy integral (10.34) takes values $-\infty < I(q) \leq \infty$. If the infimum of the energy integral is infinitely large, then by definition the logarithmic capacity is equal to zero. Suppose that $C_l(\Gamma) > 0$ and thus $-\infty < I(q) < \infty$. It is proven in Hille[8] (p. 282) that for each boundary Γ, there exists a unique minimizer q_e of $I(q)$, i.e.

$$I(q_e) = \inf_q I(q) = -\log C_l(\Gamma) \text{ with } \int_\Gamma q_e(\boldsymbol{r}) d\Gamma_r = 1. \tag{10.41}$$

For the minimizer q_e, the following result in Hille[8] (p. 287) is proven. Let Γ be the boundary of a closed bounded domain with positive logarithmic capacity and a connected complement. Then $2\pi\mathcal{K}^s q_e \leq -\log C_l(\Gamma)$ in the whole plane and $2\pi\mathcal{K}^s q_e = -\log C_l(\Gamma)$ at Γ, except possibly for a subset which has zero logarithmic capacity. ■

Theorem 10.3 leads to the following result.

Corollary 10.1. *If $C_l(\Gamma) = 1$, there exists a nonzero q_e such that $\mathcal{K}^s q_e = 0$.*

Thus in the specific case that $C_l(\Gamma) = 1$, the single layer operator $\mathcal{K}^s$ admits an eigenfunction q_e with zero eigenvalue. Hence, $\mathcal{K}^s$ is not positive definite and the Dirichlet problem does not have a unique solution.

If the BIE does not have a unique solution, we may expect that its discrete counterpart, the linear system, also does not have a unique solution.

That is, the linear system is singular, or at least ill-conditioned. This is reflected by the condition number of the system matrix, as shown in Figs. 10.5 and 10.6. Here, the condition number of the BEM matrix is plotted for two problems: the Laplace equation with Dirichlet conditions on a triangular and an ellipsoidal domain. The triangle is an isosceles right-angled triangle with sides of length l. For such a triangle the logarithmic capacity is given by

$$C_l(\text{triangle}) = \frac{3^{3/4}\Gamma^2(1/4)}{2^{7/2}\pi^{3/2}}\, l \approx 0.476\, l. \tag{10.42}$$

This implies that the condition number will be large when the scaling parameter l is close to the critical scaling $l^* := 1/0.476 \approx 2.1$. The ellipse has semi-axes of length a and $a/2$, which has a logarithmic capacity equal to $3a/4$. Hence, we may expect a large condition number when the scaling parameter a is close to $a^* := 4/3$. We observe that the condition number for the Dirichlet case (solid line) is indeed infinitely large for these two critical scalings.

If we rescale the domain such that the Euclidean diameter is smaller than one, then the second property in Section 10.5.1 shows us that the logarithmic capacity will also be smaller than one. In this way we can guarantee a unique solution of the BIE and thus a low condition number.

Recall that the non-trivial solution q_e of the homogeneous BIE $\mathcal{K}^s q = 0$ has a contour integral equal to 1. At the same time we realize that a solution q of $\mathcal{K}^s q = 0$ has to satisfy

$$\int_\Gamma q d\Gamma = \int_\Omega \Delta u d\Omega = 0, \tag{10.43}$$

where we make use of Gauss' theorem. By supplementing this requirement for q to the BIE, we exclude the possibility that q_e is a solution of the homogeneous BIE. This provides a second strategy to ensure unique solutions of the BIE.

A third option to guarantee a unique solution is to adjust the integral operator $\mathcal{K}^s$. Note that the function G_α,

$$G_\alpha(\boldsymbol{r};\boldsymbol{r}') := \frac{1}{2\pi}\log\frac{\alpha}{\|\boldsymbol{r}-\boldsymbol{r}'\|}, \quad \alpha \in \mathbb{R}^+, \tag{10.44}$$

is also a fundamental solution for the Laplace operator. The corresponding single layer potential reads

$$\mathcal{K}^s_\alpha q := \frac{1}{2\pi}\int_\Gamma \log\frac{\alpha}{\|\boldsymbol{r}-\boldsymbol{r}'\|} q(\boldsymbol{r}')d\Gamma_{\boldsymbol{r}'} = \mathcal{K}^s q + \frac{\log\alpha}{2\pi}\int_\Gamma q d\Gamma. \tag{10.45}$$

For the minimizer q_e we get

$$\mathcal{K}_\alpha^s q_e = \mathcal{K}^s q_e + \frac{\log\alpha}{2\pi}\int_\Gamma q_e d\Gamma = -\frac{1}{2\pi}\log C_l(\Gamma) + \frac{1}{2\pi}\log\alpha$$
$$= \frac{1}{2\pi}\log\frac{\alpha}{C_l(\Gamma)}. \tag{10.46}$$

This is only equal to zero if $\alpha = C_l(\Gamma)$. We may choose for α any positive real number unequal to $C_l(\Gamma)$ and obtain $\mathcal{K}_\alpha^s q_e \neq 0$. In that case, q_e is no longer an eigenfunction of the single layer potential operator with zero eigenvalue. Hence, the BIE (10.2) with Dirichlet conditions is uniquely solvable if $\mathcal{K}^s$ is replaced by $\mathcal{K}_\alpha^s$.[19,21] The advantage of this procedure is that we do not need to rescale the domain or add an extra equation. Furthermore, we do not need to know the logarithmic capacity explicitly: a rough estimate of the capacity suffices to choose α such that $\alpha \neq C_l(\Gamma)$.

There are also ways to ensure a unique solution of the BIE for the Laplace equation that can be used without having to know the logarithmic capacity. For instance, adding an extra collocation node at the interior or exterior of the domain can change the BIE in such a way that it is not singular any longer[22]; although this does depend on the location of the extra collocation node. Another option is to use the hypersingular formulation of the BIE.[23] The hypersingular BIE is the normal derivative of the standard BIE and does not involve the single layer operator. As a consequence, the BIE does not become singular at certain domains.

10.5.3. *Mixed problem*

We consider the Laplace equation with mixed boundary conditions,

$$\begin{aligned} \nabla^2 u &= 0, \quad \boldsymbol{r} \in \Omega, \\ u &= \tilde{u}, \quad \boldsymbol{r} \in \Gamma_1, \\ q &= \tilde{q}, \quad \boldsymbol{r} \in \Gamma_2, \end{aligned} \tag{10.47}$$

where $\Gamma = \Gamma_1 \cup \Gamma_2$. To investigate this boundary value problem we have to rewrite the BIE in (10.2). For $i = 1, 2$, we introduce the functions $u_i := u|_{\Gamma_i}$ and $q_i := q|_{\Gamma_i}$ and the boundary integral operators

$$(\mathcal{K}_i^s q)(\boldsymbol{r}) := \int_{\Gamma_i} G(\boldsymbol{r};\boldsymbol{r}')q(\boldsymbol{r}')d\Gamma_{r'}, \quad \boldsymbol{r} \in \Gamma, \tag{10.48a}$$

$$(\mathcal{K}_i^d u)(\boldsymbol{r}) := \int_{\Gamma_i} \frac{\partial}{\partial n_y} G(\boldsymbol{r};\boldsymbol{r}')u(\boldsymbol{r}')d\Gamma_{r'}, \quad \boldsymbol{r} \in \Gamma. \tag{10.48b}$$

Note that the boundary conditions in (10.47) provide $u_1 = \tilde{u}$ and $q_2 = \tilde{q}$. By distinguishing $\boldsymbol{r} \in \Gamma_1$ and $\boldsymbol{r} \in \Gamma_2$, we write (10.2) as a system of two BIEs,

$$\mathcal{K}_2^d u_2 - \mathcal{K}_1^s q_1 = \mathcal{K}_2^s \tilde{q} - \frac{1}{2}\tilde{u} - \mathcal{K}_1^d \tilde{u}, \quad \boldsymbol{r} \in \Gamma_1, \tag{10.49a}$$

$$\frac{1}{2}u_2 + \mathcal{K}_2^d u_2 - \mathcal{K}_1^s q_1 = \mathcal{K}_2^s \tilde{q} - \mathcal{K}_1^d \tilde{u}, \quad \boldsymbol{r} \in \Gamma_2. \tag{10.49b}$$

In this system, all prescribed boundary data are at the right-hand side of the equations.

Theorem 10.4. *If $C_l(\Gamma) = 1$, the homogeneous equations of (10.49a) and (10.49b) have a non-trivial solution pair (q_1, u_2).*

Sketch of proof. We have to find a non-trivial pair of functions (q_1, u_2) such that the left-hand sides of (10.49a) and (10.49b) are equal to zero when $C_l(\Gamma) = 1$. It can be shown that such a pair of functions exists by using information from the Dirichlet problem.[11] ■

Theorem 10.4 tells us that the BIE for the mixed problem does not have a unique solution when $C_l(\Gamma) = 1$, i.e. the BIE is singular. Moreover the division of Γ into a part Γ_1 with Dirichlet conditions and a part Γ_2 with Neumann conditions does not play a role in this. It does not make a difference whether we take Γ_1 very small or very large; the singular BIE relates solely to the whole boundary Γ.

In Figs. 10.5 and 10.6, we observe that indeed the condition number for the mixed problems is infinitely large at (almost) the same scalings as for the Dirichlet problems, agreeing with the theory. The small difference that is present is caused by numerical inaccuracies due to the discretization.

To guarantee a unique solution for the mixed problem, we have the same options as for the Dirichlet problem. The simplest remedy is to rescale the domain, thus avoiding a unit logarithmic capacity. A second option is to demand that the function q have a zero contour integral. Since part of q is already prescribed, this yields the following condition for the unknown part of q,

$$\int_{\Gamma_1} q_1 d\Gamma = -\int_{\Gamma_2} \tilde{q} d\Gamma. \tag{10.50}$$

As a last option to obtain nonsingular BIEs, we can also replace the single layer operator $\mathcal{K}^s$ by $\mathcal{K}_\alpha^s$ (see Section 10.5.2).

10.6. Condition Numbers in Flow Problems

The Laplace equation and the Stokes equations have at least one thing in common: the Laplace operator appears in both equations. As we have seen in the previous section, the Laplace equation may lead to a singular BIE for certain critical domains. The question arises whether this is also the case for the equations in viscous flow problems: can the corresponding BIEs become singular on certain critical domains?

In this section, we study the BIEs following from the Stokes equations. In particular, we focus on the eigenvalues of the integral operators. It is shown that for certain critical domains these integral operators admit zero eigenvalues. Hence, again we find that the BIEs become singular for a number of critical domains.

For the Laplace equation, it is possible to *a priori* determine the critical domains. For a number of simple domains, the logarithmic capacity can be used to exactly compute the critical size. For more involved domains, the logarithmic capacity can be used to estimate the critical size of the domain. Unfortunately, the critical domains for the Stokes equations do not coincide with the critical domains for the Laplace equations. Hence, we cannot use the logarithmic capacity to *a priori* determine the critical domains on which the BIEs for Stokes equations become singular. It is only by numerical experiments that we can distinguish the critical domains.

Let Ω be a two-dimensional simply-connected domain with a piece-wise smooth boundary Γ. The Stokes equations for a viscous flow in Ω read

$$\begin{aligned} \nabla^2 \boldsymbol{v} - \nabla p &= \mathbf{0}, \\ \nabla . \boldsymbol{v} &= 0, \end{aligned} \tag{10.51}$$

where $\boldsymbol{v}$ is the velocity field of the fluid and p its pressure. Let Γ be divided into a part Γ_1 on which the velocity $\boldsymbol{v}$ is prescribed, and a part Γ_2 on which the pressure p is prescribed, $\Gamma = \Gamma_1 \bigcup \Gamma_2$. Hence, the Stokes equations are subject to the boundary conditions

$$\begin{aligned} \boldsymbol{v} &= \tilde{\boldsymbol{v}}, \quad \boldsymbol{r} \in \Gamma_1, \\ p &= \tilde{p}, \quad \boldsymbol{r} \in \Gamma_2. \end{aligned} \tag{10.52}$$

Either Γ_1 or Γ_2 can be empty, leading to a purely Neumann or Dirichlet problem, respectively. The Stokes equations in differential form can be

transformed to a set of two BIEs:[6,24,25]

$$\frac{1}{2}v_i(\boldsymbol{r}) + \int_\Gamma q_{ij}(\boldsymbol{r},\boldsymbol{r}')v_j(\boldsymbol{r}')d\Gamma_{r'} = \int_\Gamma u_{ij}(\boldsymbol{r},\boldsymbol{r}')b_j(\boldsymbol{r}')d\Gamma_{r'}, \quad \boldsymbol{r}\in\Gamma,\ i=1,2. \tag{10.53}$$

Here, a repeated index means summation over all possible values of that index. The vector function $\boldsymbol{b}$ is the normal stress at the fluid boundary,

$$\boldsymbol{b} := \sigma(p,\boldsymbol{v})\boldsymbol{n}, \tag{10.54}$$

with $\boldsymbol{n}$ being the outward unit normal at the boundary and the stress tensor σ being defined by

$$\sigma_{ij}(p,\boldsymbol{v}) := -p\delta_{ij} + \Big(\frac{\partial v_i}{\partial x_j} + \frac{\partial v_j}{\partial x_i}\Big). \tag{10.55}$$

Hence, the boundary integral formulation involves two variables: the velocity $\boldsymbol{v}$ and the normal stress $\boldsymbol{b}$. In correspondence to (10.52), at each point of the boundary either $\boldsymbol{v}$ or $\boldsymbol{b}$ is prescribed:

$$\begin{aligned} \boldsymbol{v} &= \tilde{\boldsymbol{v}}, && \boldsymbol{r}\in\Gamma_1,\\ \boldsymbol{b} &= -\tilde{p}\boldsymbol{n}, && \boldsymbol{r}\in\Gamma_2. \end{aligned} \tag{10.56}$$

The kernels u_{ij} and q_{ij} in the integral operators are defined as

$$\begin{aligned} q_{ij}(\boldsymbol{r},\boldsymbol{r}') &:= \frac{1}{\pi}\frac{(x_i-y_i)(x_j-y_j)(x_k-y_k)n_k}{\|\boldsymbol{r}-\boldsymbol{r}'\|^4},\\ u_{ij}(\boldsymbol{r},\boldsymbol{r}') &:= \frac{1}{4\pi}\left\{\delta_{ij}\log\frac{1}{\|\boldsymbol{r}-\boldsymbol{r}'\|} + \frac{(x_i-y_i)(x_j-y_j)}{\|\boldsymbol{r}-\boldsymbol{r}'\|^2}\right\}, \end{aligned} \tag{10.57}$$

for $i,j=1,2$. We introduce boundary integral operators,

$$\begin{aligned} (\mathcal{G}\varphi)_i(\boldsymbol{r}) &:= \int_\Gamma u_{ij}(\boldsymbol{r},\boldsymbol{r}')\varphi_j(\boldsymbol{r}')d\Gamma_{r'},\\ (\mathcal{H}\psi)_i(\boldsymbol{r}) &:= \int_\Gamma q_{ij}(\boldsymbol{r},\boldsymbol{r}')\psi_j(\boldsymbol{r}')d\Gamma_{r'}, \end{aligned} \tag{10.58}$$

which enables us to write (10.53) as

$$\Big(\frac{1}{2}\mathcal{I}+\mathcal{H}\Big)\boldsymbol{v} = \mathcal{G}\boldsymbol{b}. \tag{10.59}$$

The operators $\mathcal{G}$ and $\mathcal{H}$ are called the *single and double layer operator* for the Stokes equations. For the Dirichlet problem, the velocity $\boldsymbol{v}$ at the

boundary is given ($\Gamma_2 = \emptyset$) and we would like to reconstruct the normal stress $\boldsymbol{b}$ at the boundary. To this end, we need to invert the operator $\mathcal{G}$. This can only be done when all eigenvalues of $\mathcal{G}$ are unequal to zero. In this section we investigate the conditions under which $\mathcal{G}$ admits a zero eigenvalue.

For the mixed problem, the velocity at Γ_1 is prescribed and the normal stress at Γ_2 is prescribed. We would like to reconstruct the unknown velocity at Γ_2 and the unknown normal stress at Γ_1. After rearranging known and unknown terms (see Section 10.6.2) we again need to invert a boundary integral operator. This can only be done when all eigenvalues of the operator are unequal to zero. We will show that zero eigenvalues occur under the same conditions as for the Dirichlet problem.

10.6.1. *Flow problems with dirichlet boundary conditions*

In this subsection, we study the solvability of the BIE (10.59) with Dirichlet conditions on a piece-wise smooth closed boundary Γ. We search for eigenfunctions $\boldsymbol{b}$ of the boundary integral operator $\mathcal{G}$ with zero eigenvalue, hence $\mathcal{G}\boldsymbol{b} = 0$. If such eigenfunctions exist, the boundary integral operator $\mathcal{G}$ is not invertible and the integral equation (10.59) is not uniquely solvable. First, we show that at least one such eigenfunction with zero eigenvalue exists.

Theorem 10.5. *For any smooth boundary Γ, the outward unit normal $\boldsymbol{n}(\boldsymbol{r})$ is an eigenfunction of the boundary integral operator $\mathcal{G}$ with eigenvalue zero.*

Proof. The i-th component of $\mathcal{G}\boldsymbol{n}$ equals

$$\begin{aligned}(\mathcal{G}\boldsymbol{n})_i &= \int_\Gamma u_{ij}(\boldsymbol{r},\boldsymbol{r}')n_j(\boldsymbol{r}')d\Gamma_{r'} \\ &= \frac{1}{4\pi}\int_\Gamma \left[\delta_{ij}\log\frac{1}{\|\boldsymbol{r}-\boldsymbol{r}'\|} + \frac{(x_i-y_i)(x_j-y_j)}{\|\boldsymbol{r}-\boldsymbol{r}'\|^2}\right] n_j(\boldsymbol{r}')d\Gamma_{r'} \\ &= \frac{1}{4\pi}\int_\Omega \frac{\partial}{\partial x_j}\left[\delta_{ij}\log\frac{1}{\|\boldsymbol{r}-\boldsymbol{r}'\|} + \frac{(x_i-y_i)(x_j-y_j)}{\|\boldsymbol{r}-\boldsymbol{r}'\|^2}\right] d\Omega_y \\ &= -\int_\Omega \frac{\partial}{\partial x_j}u_j^i d\Omega_y = -\int_\Omega \nabla.\boldsymbol{u}^i d\Omega = 0. \end{aligned} \tag{10.60}$$

Here, the vector $\boldsymbol{u}^i$ is the velocity due to a Stokeslet,[24] i.e. the velocity field induced by a point force in the $\boldsymbol{e}_i$-direction. This velocity field satisfies the incompressibility condition $\nabla.\boldsymbol{u}^i = 0$. □

In the sequel to this section, we assume that the solutions of the Dirichlet problem (10.59) are sought in a function space that excludes the normal. Hence, the eigenfunctions $\boldsymbol{b}$ of $\mathcal{G}$ we are looking for are perpendicular to $\boldsymbol{n}$.

We now show that for each boundary Γ there exist (at most) two critical scalings of the boundary such that the operator $\mathcal{G}$ in the Dirichlet problem (10.59) is not invertible. This phenomenon has been observed and proven[26] and we will partly present the analysis here. The scaling for which the operator $\mathcal{G}$ is not invertible is called a *critical scaling*, and the corresponding boundary a *critical boundary*. The domain that is enclosed by the critical boundary is referred to as the *critical domain*.

Theorem 10.6. *For all given functions* $\boldsymbol{f}$ *and constant vectors* $\boldsymbol{d}$ *the system of equations*

$$\begin{cases} \mathcal{G}\boldsymbol{b} + \boldsymbol{c} = \boldsymbol{f}, \\ \int_\Gamma \boldsymbol{b} d\Gamma = \boldsymbol{d}, \end{cases} \tag{10.61}$$

has a unique solution pair $(\boldsymbol{b}, \boldsymbol{c})$*, where* $\boldsymbol{b}$ *is a function and* $\boldsymbol{c}$ *is a constant vector.*

Sketch of proof. The main idea is to show that the operator that maps the pair $(\boldsymbol{b}, \boldsymbol{c})$ to the left-hand side of (10.61) is an isomorphism.[26] ■

We proceed by introducing the two unit vectors $\boldsymbol{e}_1 = [1, 0]^T$ and $\boldsymbol{e}_2 = [0, 1]^T$. Theorem 10.6 guarantees that two pairs $(\boldsymbol{b}^1, \boldsymbol{c}^1)$ and $(\boldsymbol{b}^2, \boldsymbol{c}^2)$ exist that are the unique solutions to the two systems

$$\begin{cases} \mathcal{G}\boldsymbol{b}^1 + \boldsymbol{c}^1 = \boldsymbol{0}, \\ \int_\Gamma \boldsymbol{b}^1 d\Gamma = \boldsymbol{e}_1, \end{cases} \quad \begin{cases} \mathcal{G}\boldsymbol{b}^2 + \boldsymbol{c}^2 = \boldsymbol{0}, \\ \int_\Gamma \boldsymbol{b}^2 d\Gamma = \boldsymbol{e}_2. \end{cases} \tag{10.62}$$

We define the matrix $\mathbf{C}_\Gamma$ as $\mathbf{C}_\Gamma := [\boldsymbol{c}^1 | \boldsymbol{c}^2]$.

Theorem 10.7. *If* $\det(\mathbf{C}_\Gamma) = 0$*, then the operator* $\mathcal{G}$ *is not invertible.*

Proof. Suppose that $\det(\mathbf{C}_\Gamma) = 0$, then the columns $\boldsymbol{c}^1$ and $\boldsymbol{c}^2$ are dependent, say $\boldsymbol{c}^1 = \alpha \boldsymbol{c}^2$ for some $\alpha \in \mathbb{R}$, $\alpha \neq 0$. In that case

$$\begin{aligned} \boldsymbol{0} &= \left(\mathcal{G}\boldsymbol{b}^1 + \boldsymbol{c}^1\right) - \alpha \left(\mathcal{G}\boldsymbol{b}^2 + \boldsymbol{c}^2\right) \\ &= \mathcal{G}(\boldsymbol{b}^1 - \alpha \boldsymbol{b}^2) + \alpha \boldsymbol{c}^2 - \alpha \boldsymbol{c}^2 \\ &= \mathcal{G}(\boldsymbol{b}^1 - \alpha \boldsymbol{b}^2). \end{aligned} \tag{10.63}$$

The function $\boldsymbol{b}^1 - \alpha \boldsymbol{b}^2$ cannot be equal to zero, since this requires $\int_\Gamma (\boldsymbol{b}^1 - \alpha \boldsymbol{b}^2) d\Gamma$ to be equal to zero, while we have

$$\int_\Gamma (\boldsymbol{b}^1 - \alpha \boldsymbol{b}^2) d\Gamma = \boldsymbol{e}_1 - \alpha \boldsymbol{e}_2 \neq \boldsymbol{0}. \tag{10.64}$$

So $\boldsymbol{b}^1 - \alpha \boldsymbol{b}^2$ is an eigenfunction of $\mathcal{G}$ with zero eigenvalue. This eigenfunction cannot be equal to the normal $\boldsymbol{n}$, since $\boldsymbol{n}$ also requires $\int_\Gamma \boldsymbol{n} d\Gamma = 0$. □

Corollary 10.2. *There are (at most) two critical scalings of the domain Γ for which the operator $\mathcal{G}$ is not invertible.*

Proof. We rescale the domain Γ by a factor a, i.e. $\Gamma \to a\Gamma$. With the definition of the operator $\mathcal{G}$, it can be shown that

$$\mathcal{G}\boldsymbol{b} \to \mathcal{G}^a \boldsymbol{b} := -\frac{1}{4\pi} \int_\Gamma a \log a \; \boldsymbol{b} d\Gamma + a\mathcal{G}\boldsymbol{b}. \tag{10.65}$$

Then the two systems in (10.62) change into

$$\begin{cases} a\mathcal{G}\boldsymbol{b}^j + \boldsymbol{c}^j - \frac{1}{4\pi} \int_\Gamma a \log a \; \boldsymbol{b}^j d\Gamma = \boldsymbol{0}, \\ a \int_\Gamma \boldsymbol{b}^j d\Gamma = \boldsymbol{e}_j, \; j = 1, 2. \end{cases} \tag{10.66}$$

In defining $\boldsymbol{b}_a^j := a\boldsymbol{b}^j$ for $j = 1, 2$, we obtain

$$\begin{cases} \mathcal{G}\boldsymbol{b}_a^j + \boldsymbol{c}^j - \frac{1}{4\pi} \int_\Gamma \log a \; \boldsymbol{b}_a^j d\Gamma = \boldsymbol{0}, \\ \int_\Gamma \boldsymbol{b}_a^j d\Gamma = \boldsymbol{e}_j, \; j = 1, 2. \end{cases} \tag{10.67}$$

Substituting the second equation into the first equation, we get

$$\begin{cases} \mathcal{G}\boldsymbol{b}_a^j + \boldsymbol{c}^j - \frac{1}{4\pi} \log a \; \boldsymbol{e}_j = \boldsymbol{0}, \\ \int_\Gamma \boldsymbol{b}_a^j d\Gamma = \boldsymbol{e}_j, \; j = 1, 2. \end{cases} \tag{10.68}$$

These systems have the same form as the original systems in (10.62), except for the change $\boldsymbol{c}^j \to \boldsymbol{c}^j - \frac{1}{4\pi} \log a \; \boldsymbol{e}_j$ for $j = 1, 2$. Define the new matrix $\mathbf{C}_{a\Gamma}$ by

$$\mathbf{C}_{a\Gamma} := \mathbf{C}_\Gamma - \frac{1}{4\pi} \log a \; \mathbf{I}_2, \tag{10.69}$$

then $\mathcal{G}^a$ is not invertible when $\det(\mathbf{C}_{a\Gamma}) = 0$. Hence, when $\frac{1}{4\pi} \log a$ is an eigenvalue of $\mathbf{C}_\Gamma$, the operator $\mathcal{G}^a$ is not invertible. This implies that when $\mathbf{C}_\Gamma$ has two distinct eigenvalues, there are two critical scalings a for which $\mathcal{G}^a$ is not invertible. If $\mathbf{C}_\Gamma$ has one eigenvalue with double multiplicity these critical scalings coincide. □

The result of corollary 10.2 shows that the BIEs for the Dirichlet Stokes equations become singular for certain sizes of the domain. As a consequence, the equations are not uniquely solvable. This solvability problem is an artifact of the boundary integral formulation: the Stokes equations in differential form always have a unique solution. In the previous section, a similar phenomenon was observed for the Laplace equation with Dirichlet conditions; in its differential form, the problem is well-posed, while the corresponding BIE is not solvable at critical boundaries.

For the Laplace equation, the critical scaling is related to the logarithmic capacity of the domain. By calculating or estimating the logarithmic capacity one can determine or estimate the critical domains without computing BEM matrices and evaluating their condition numbers. It is this *a priori* information that allows us to modify the standard BEM formulation such that the BIE becomes uniquely solvable.

For the Stokes equations, there does not exist an equivalent to the logarithmic capacity. Hence we cannot *a priori* determine the critical domains. One way to determine the critical domains is by computing the BEM-matrices and evaluating their condition numbers. If the condition number jumps to infinity for a certain domain, then this domain is a critical domain. Hence, this strategy requires the solution of many BEM problems.

Another possibility for determining the critical domains is by solving the systems in (10.62). This yields the matrix $\mathbf{C}_\Gamma$ and, subsequently, the matrix $\mathbf{C}_{a\Gamma}$. By calculating the eigenvalues of the latter matrix, the critical scalings can be found. Again, we have to solve two non-standard BEM problems to compute the critical scalings.

Remark. The BIEs for the Stokes flow in 2D are similar to the equations for plane elasticity. Hence, the BIEs for the latter equations suffer from the same solvability problems as the Stokes equations. A proof of this phenomenon for plane elasticity is found in the literature[27] and is similar to the proof sketched above.

10.6.2. *Flow problems with mixed boundary conditions*

In the previous subsection, we showed that the boundary integral operator $\mathcal{G}$ for the Dirichlet Stokes equations is not invertible for all domains. In this subsection, we will show that this phenomenon extends to the Stokes equations with mixed boundary conditions.

The starting point is again the BIE for the Stokes equations,

$$\frac{1}{2}\boldsymbol{v} + \mathcal{H}\boldsymbol{v} = \mathcal{G}\boldsymbol{b}, \text{ at } \Gamma. \tag{10.70}$$

Suppose that the boundary Γ is split into two parts, $\Gamma = \Gamma_1 \bigcup \Gamma_2$. On Γ_1, we prescribe the velocity $\boldsymbol{v}^1$ while the normal stress $\boldsymbol{b}^1$ is unknown. On Γ_2, we prescribe the normal stress $\boldsymbol{b}^2$ while the velocity $\boldsymbol{v}^2$ is unknown. The boundary integral operators $\mathcal{G}$ and $\mathcal{H}$ are split accordingly,

$$\begin{aligned}
[\mathcal{G}\boldsymbol{b}]_i &= \int_\Gamma u_{ij} b_j d\Gamma = \int_{\Gamma_1} u_{ij} b_j^1 d\Gamma + \int_{\Gamma_2} u_{ij} b_j^2 d\Gamma =: [\mathcal{G}^1 \boldsymbol{b}^1]_i + [\mathcal{G}^2 \boldsymbol{b}^2]_i, \\
[\mathcal{H}\boldsymbol{v}]_i &= \int_\Gamma q_{ij} v_j d\Gamma = \int_{\Gamma_1} q_{ij} v_j^1 d\Gamma + \int_{\Gamma_2} q_{ij} v_j^2 d\Gamma =: [\mathcal{H}^1 \boldsymbol{v}^1]_i + [\mathcal{H}^2 \boldsymbol{v}^2]_i.
\end{aligned} \tag{10.71}$$

With these notations, the BIE is written in the following way:

$$\frac{1}{2}\boldsymbol{v}^k + \mathcal{H}^1\boldsymbol{v}^1 + \mathcal{H}^2\boldsymbol{v}^2 = \mathcal{G}^1\boldsymbol{b}^1 + \mathcal{G}^2\boldsymbol{b}^2, \quad \text{at } \Gamma_k, \ k = 1, 2. \tag{10.72}$$

We arrange the terms in such a way that all unknowns are at the left-hand side and all knowns are at the right-hand side,

$$\begin{aligned}
\mathcal{H}^2\boldsymbol{v}^2 - \mathcal{G}^1\boldsymbol{b}^1 &= \mathcal{G}^2\boldsymbol{b}^2 - \mathcal{H}^1\boldsymbol{v}^1 - \frac{1}{2}\boldsymbol{v}^1, \quad \text{at } \Gamma_1, \\
\frac{1}{2}\boldsymbol{v}^2 + \mathcal{H}^2\boldsymbol{v}^2 - \mathcal{G}^1\boldsymbol{b}^1 &= \mathcal{G}^2\boldsymbol{b}^2 - \mathcal{H}^1\boldsymbol{v}^1, \quad \text{at } \Gamma_2.
\end{aligned} \tag{10.73}$$

Now we can define an operator $\mathcal{A}$ that assigns to the pair $(\boldsymbol{b}^1, \boldsymbol{v}^2)$ the two functions at the left-hand side of (10.73),

$$\begin{bmatrix} \boldsymbol{b}^1 \\ \boldsymbol{v}^2 \end{bmatrix} \xrightarrow{\mathcal{A}} \begin{bmatrix} \mathcal{H}^2\boldsymbol{v}^2 - \mathcal{G}^1\boldsymbol{b}^1 \\ \frac{1}{2}\boldsymbol{v}^2 + \mathcal{H}^2\boldsymbol{v}^2 - \mathcal{G}^1\boldsymbol{b}^1 \end{bmatrix} \tag{10.74}$$

To study the invertibility of this operator, we need to study the homogeneous version of the eqs in (10.73),

$$\begin{aligned}
\mathcal{H}^2\boldsymbol{v}^2 - \mathcal{G}^1\boldsymbol{b}^1 &= 0, \quad \text{at } \Gamma_1, \\
\frac{1}{2}\boldsymbol{v}^2 + \mathcal{H}^2\boldsymbol{v}^2 - \mathcal{G}^1\boldsymbol{b}^1 &= 0, \quad \text{at } \Gamma_2.
\end{aligned} \tag{10.75}$$

Theorem 10.8. *There are (at most) two scalings of Γ such that the homogeneous eqs in (10.75) have a non-trivial solution, i.e. $\mathcal{A}$ is not invertible.*

Sketch of proof. We have to find a non-trivial pair of functions $(\boldsymbol{b}_1, \boldsymbol{v}_2)$ such that the left-hand sides of (10.75) are equal to zero when $C_l(\Gamma) = 1$. Similar to the Laplacian case, it can be shown that such a pair of functions exists by using information from the Dirichlet problem.[28] ■

This result shows that the BIE for the Stokes equations with mixed boundary conditions may also become singular. This happens for the same critical boundaries as for the Stokes equations with Dirichlet boundary conditions. Hence, the mixed problem inherits the singularities from the Dirichlet problem. The division of the boundary into a Dirichlet and a Neumann part does not play a role in this.

Note that the Laplace equation exhibits the same behaviour. The boundary integral equation for the Laplace equation with mixed boundary conditions also inherits the solvability problems from the BIE for the Dirichlet case.[11]

10.6.3. *Numerical examples*

To solve the BIEs (10.59), the boundary Γ is discretized into a set of N linear elements. At each element, the velocity $\boldsymbol{v}$ and normal stress $\boldsymbol{b}$ are approximated linearly. In this way, the BIEs are transformed into a linear system of algebraic equations. (For details about the discretization, refer to any BEM handbook.[29,30]) We introduce vectors $\mathbf{v}$ and $\mathbf{b}$ of length $2N$ containing the coefficients of $\boldsymbol{v}$ and $\boldsymbol{b}$ at the nodal points. Then the system of equations can be written in short-hand notation as

$$\mathbf{G}\mathbf{b} = \left(\frac{1}{2}\mathbf{I} + \mathbf{H}\right)\mathbf{v}. \tag{10.76}$$

Here, $\mathbf{G}$ and $\mathbf{H}$ are the discrete counterparts of the single and double layer operator.

If the boundary integral operator $\mathcal{G}$ is not invertible, then its discrete counterpart, the matrix $\mathbf{G}$, is ill-conditioned. To visualize this, we compute the condition number of $\mathbf{G}$: if the condition number is infinitely large, then the matrix is not invertible. As a consequence, the linear system (10.76) is singular and cannot be solved for arbitrary right-hand side vectors. If the condition number is bounded but very large, then the problem (10.76) is still difficult to solve accurately.

In the following examples, we construct the matrix $\mathbf{G}$ for a certain boundary Γ and compute the condition number of this matrix. Then

we rescale the boundary Γ by a factor a, i.e. $\Gamma \rightarrow a\Gamma$. Again, we compute the condition number of the matrix $\mathbf{G}$. We do this for several values of the scaling parameter a. According to the theory in the previous sections, there are two critical scalings for which the integral operator $\mathcal{G}$ is not invertible. For these two scalings the matrix $\mathbf{G}$ is not invertible, or at least very ill-conditioned. Hence, we expect that the condition number of $\mathbf{G}$ will jump to infinity at these two scalings. The scaling for which such large condition numbers appear is called a *critical scaling* and has, ideally, the same value as the critical scaling defined for the BIE in the previous section. However, due to the discretization of the equations, the critical scaling for the discrete problem may be slightly different from the critical scaling for the BIE. In the limit $N \rightarrow \infty$ these differences vanish.

As the results for the Dirichlet and mixed problems are similar, we do not present any examples for the mixed case here.

Example 10.6.1. In Fig. 10.7, we show the condition number as a function of the scale a. We do this for an ellipse (ellipse 1) with aspect ratio 0.4 and for an ellipse (ellipse 2) with aspect ratio 0.7. We observe that for both cases two critical scalings exist for which the condition number goes to infinity. Moreover, these critical scalings differ significantly for the two ellipses. For ellipse 1, we find critical scalings 1.9 and 2.9 approximately, while for ellipse 2 we find 1.8 and 2.1. Hence the shape of the ellipse, i.e. its aspect ratio, greatly influences the values of the critical scalings.

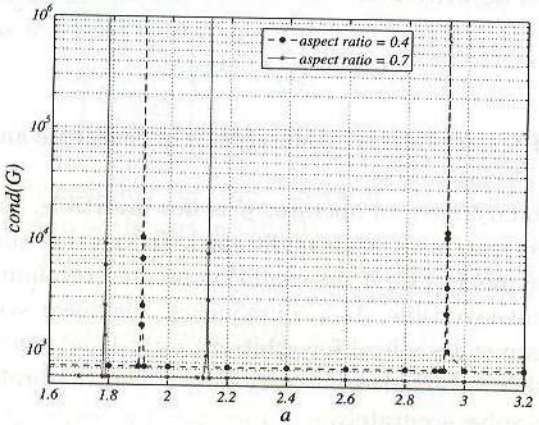

Fig. 10.7. Condition number of $\mathbf{G}$ for an ellipsoidal domain with aspect ratios 0.4 and 0.7 as a function of scaling parameter a.

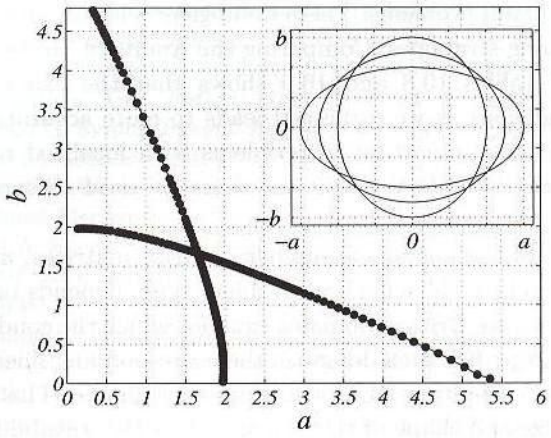

Fig. 10.8. The critical sizes of an ellipse for which the condition number of **G** is very large.

Figure 10.8 visualizes all ellipses for which the condition number of **G** is very large, i.e. all critical ellipses with different aspect ratios. At the horizontal axis is the length a of the horizontal semi-axis of the ellipse, at the vertical axis is the length b of the vertical semi-axis of the ellipse. We compute the condition number of **G** for several values of a and b. We call the values of a and b for which the condition number goes to infinity the *critical sizes* and the corresponding ellipse the critical ellipse. At the *critical sizes* we plot a dot in the (a, b)-plane of Fig. 10.8. We see that the critical sizes lie on two curved lines, which are symmetric around the line $a = b$. It can be concluded that for an ellipse with fixed aspect ratio $d := a/b \neq 1$, two critical sizes exist. For a circle, where $d = 1$, only one critical size exists. The values corresponding to this critical size are approximately $a = b = 1.65$, which agrees with the critical scale $\exp(1/2) \approx 1.649$ that can be derived analytically.[28]

10.7. Discussion

In this chapter, we have looked at the fundamental causes of error in the BEM and provided expressions for local errors. A proper definition of error will be at the core of any adaptive grid refinement strategy. We have shown that the local error for both constant and linear elements is of quadratic order. This is confirmed by the results in Tables 10.1 to 10.3. These results plus those in Table 10.4 show that this error behaviour holds for Dirichlet

as well as Neumann problems. These findings provide an informed guide for choosing meshing strategies. Comparing the results of Tables 10.6 and 10.7 and those of Tables 10.8 and 10.9 shows that the exact treatment of boundary conditions as we explained leads to more accurate results. This will be particularly important in problems with localized regions of high variations in the boundary condition where we need to capture the high activity.

The value of the condition number of BEM matrices, apart from the number of boundary elements and problem type, depends on the size and shape of the domain. Critical domains exist for which the condition numbers are infinitely large. For such domains, the corresponding linear systems are singular and any resulting BEM solution is not unique. This phenomenon, whereby the size and shape of the domain affect the solvability, is a typical two-dimensional problem. In three dimensions this does not occur. The core of the phenomenon is the logarithmic term in the 2D fundamental solution for the differential operators that transforms a scaling of the domain into an additive term. In three dimensions, such a logarithmic term does not appear in the fundamental solution.

We have presented a number of strategies to avoid critical domains, which can be implemented easily in existing BEM codes. This will guarantee the uniqueness of the BEM solutions for domains of all sizes and shapes.

For potential problems, one can *a priori* determine or estimate the critical domains on which the condition number of the BEM matrix is infinitely large. This is achieved by exploiting the concept of logarithmic capacity. Unfortunately, we cannot use this strategy to determine or estimate the critical domains for flow problems, since an equivalent concept of the logarithmic capacity for flow problems does not yet exist.

In this chapter, we have shown that critical domains exist for potential problems and flow problems, and at the same time critical domains occur when solving the biharmonic equation with the BEM.[31–33] The question arises whether critical domains exist for a broader class of boundary value problems. To the authors' knowledge this is still an open question.

References

1. M. Guiggiani and F. Lombardi, Self-adaptive boundary elements with h-hierachical shape functions, *Advances in Engineering Software, Special issue on error estimates and adaptive meshes for FEM/BEM* **15**, 269–277, (1992).
2. J. T. C. M. T. Liang and S. S. Yang, Error estimation for boundary element method., *Engineering Analysis with Boundary Elements* **23**, 257–265, (1999).

3. C. Carsten and E. P. Stephan, A posteriori error estimates for boundary element methods., *Mathematics of Computation* **64**, 483–500, (1995).
4. G. Hsiao, On the stability of integral equations of the first kind with logarithmic kernels, *Arch. Ration. Mech. Anal.* **94**, 179–192, (1986).
5. M. Jaswon and G. Symm, *Integral Equation Methods in Potential Theory and Elastostatics* (Academic Press, London, 1977).
6. H. Power and L. Wrobel, *Boundary Integral Methods in Fluid Mechanics*, (Computational Mechanics Publications, Southampton, 1995).
7. I. Sloan and A. Spence, The Galerkin method for integral equations of the first kind with logarithmic kernel: Theory, *IMA J. Numer. Anal.* **8**, 105–122, (1988).
8. E. Hille, *Analytic Function Theory: Vol II.* (Ginn, London, 1959).
9. N. Landkof, *Foundations of Modern Potential Theory* (Springer Verlag, Berlin, 1972).
10. M. Tsuji, *Potential Theory in Modern Function Theory* (Maruzen, Tokyo, 1959).
11. W. Dijkstra and R. Mattheij, A relation between the logarithmic capacity and the condition number of the BEM-matrices, *Comm. Numer. Methods Engrg.* **23**(7), 665–680, (2007).
12. M. T. Heath, *Scientific Computing, an Introductory Survey* (McGraw Hill, New York, 2002).
13. S. Christiansen, Condition number of matrices derived from two classes of integral equations, *Mat. Meth. Appl. Sci.* **3**, 364–392, (1981).
14. S. Christiansen, On two methods for elimination of non-unique solutions of an integral equation with logarithmic kernel, *Appl. Anal.* **13**, 1–18, (1982).
15. W. Dijkstra and R. Mattheij, The condition number of the BEM-matrix arising from Laplace's equation, *Electron. J. Bound. Elem.* 4(2), 67–81, (2006).
16. R. Barnard, K. Pearce, and A. Solynin, Area, width, and logarithmic capacity of convex sets, *Pacific J. Math.* **212**, 13–23, (2003).
17. J. Rostand, Computing logarithmic capacity with linear programming, *Experiment. Math.* **6**, 221–238, (1997).
18. W. Dijkstra and M. Hochstenbach, Numerical approximation of the logarithmic capacity, *Appl. Numer. Math.* (2008). Submitted for publication.
19. W. McLean, *Strongly Elliptic Systems and Boundary Integral Equations* (Cambridge University Press, Cambridge, 2000).
20. Y. Yan and I. Sloan, On integral equations of the first kind with logarithmic kernels, *J. Integral Equations Appl.* **1**, 549–579, (1988).
21. C. Constanda, On the solution of the Dirichlet problem for the two-dimensional Laplace equation, *Proc. Amer. Math. Soc.* **119**(3), 877–884, (1993).
22. J. Chen, C. Lee, I. Chen, and J. Lin, An alternative method for degenerate scale problems in boundary element methods for the two-dimensional Laplace equation, *Eng. Anal. Bound. Elem.* **26**, 559–569, (2002).
23. J. Chen, J. Lin, S. Kuo, and Y. Chiu, Analytical study and numerical experiments for degenerate scale problems in boundary element method

using degenerate kernels and circulants, *Eng. Anal. Bound. Elem.* **25**, 819–828, (2001).
24. O. Ladyzhenskaya, *The Mathematical Theory of Viscous Incompressible Flow.* (Gordon and Beach, New York-London, 1963).
25. C. Pozrikidis, *Boundary Integral and Singularity Methods for Linearized Viscous Flows* (Cambridge University Press, Cambridge, 1992).
26. V. Domínguez and F. Sayas, A BEM-FEM overlapping algorithm for the Stokes equation, *Appl. Math. Comput.* **182**, 691–710, (2006).
27. R. Vodička and V. Mantič, On invertibility of elastic single-layer potential operator, *J. Elasticity.* **74**, 147–173, (2004).
28. W. Dijkstra and R. Mattheij, Condition number of the BEM matrix arising from the Stokes equations in 2D, *Eng. Anal. Bound. Elem.* **32**(9), 736–746, (2008).
29. A. Becker, *The Boundary Element Method in Engineering* (McGraw-Hill, Maidenhead, 1992).
30. C. Brebbia, J. Telles, and L. Wrobel, *The Boundary Element Method in Engineering* (McGraw-Hill Book Company, London, 1984).
31. B. Fuglede, On a direct method of integral equations for solving the biharmonic Dirichlet problem, *ZAMM.* **61**, 449–459, (1981).
32. M. Costabel and M. Dauge, On invertibility of the biharmonic single-layer potential operator, *Integr. Equ. Oper. Theory* **24**, 46–67, (1996).
33. C. Constanda, On the Dirichlet problem for the two-dimensional biharmonic equation, *Mat. Meth. Appl. Sci.* **20**, 885–890, (1997).